

30 nm resolution x-ray imaging at 8 keV using third order diffraction of a zone plate lens objective in a transmission microscope

Gung-Chian Yin, Yen-Fang Song, Mau-Tsu Tang, Fu-Rong Chen, Keng S. Liang, Frederick W. Duewer, Michael Feser, Wenbing Yun, and Han-Ping D. Shieh

Citation: *Applied Physics Letters* **89**, 221122 (2006); doi: 10.1063/1.2397483

View online: <http://dx.doi.org/10.1063/1.2397483>

View Table of Contents: <http://scitation.aip.org/content/aip/journal/apl/89/22?ver=pdfcov>

Published by the [AIP Publishing](#)

Articles you may be interested in

Hydrogen silsesquioxane double patterning process for 12 nm resolution x-ray zone plates
J. Vac. Sci. Technol. B **27**, 2606 (2009); 10.1116/1.3242694

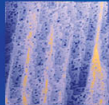
Hard-x-ray microscopy with Fresnel zone plates reaches 40 nm Rayleigh resolution
Appl. Phys. Lett. **92**, 103119 (2008); 10.1063/1.2857476

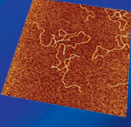
Nanofabrication of high aspect ratio 24 nm x-ray zone plates for x-ray imaging applications
J. Vac. Sci. Technol. B **25**, 2004 (2007); 10.1116/1.2789447

Energy-tunable transmission x-ray microscope for differential contrast imaging with near 60 nm resolution tomography
Appl. Phys. Lett. **88**, 241115 (2006); 10.1063/1.2211300

25 nm mechanically buttressed high aspect ratio zone plates: Fabrication and performance
J. Vac. Sci. Technol. B **22**, 3186 (2004); 10.1116/1.1815298

NEW! **Asylum Research MFP-3D Infinity™ AFM** Unmatched Performance, Versatility and Support

 **Stunning high performance**
Comprehensive tools for nanomechanics 

 **Simpler than ever to GetStarted™**
Widest range of accessories for materials science and bioscience 

OXFORD INSTRUMENTS
The Business of Science®



30 nm resolution x-ray imaging at 8 keV using third order diffraction of a zone plate lens objective in a transmission microscope

Gung-Chian Yin^{a)}

National Synchrotron Radiation Research Center, 101 Hsin-Ann Road, Hsinchu 30076, Taiwan; Department of Photonics, National Chiao Tung University, Hsinchu 300, Taiwan; and Display Institute, National Chiao Tung University, Hsinchu 300, Taiwan

Yen-Fang Song, Mau-Tsu Tang, Fu-Rong Chen, and Keng S. Liang

National Synchrotron Radiation Center, 101 Hsin-Ann Road, Hsinchu 30076, Taiwan

Frederick W. Duewer, Michael Feser, and Wenbing Yun

Xradia Inc., 5052 Commercial Circle, Concord, California 94520

Han-Ping D. Shieh

Department of Photonics, National Chiao Tung University, Hsinchu 300, Taiwan and Display Institute, National Chiao Tung University, Hsinchu 300, Taiwan

(Received 22 August 2006; accepted 22 October 2006; published online 1 December 2006)

A hard x-ray transmission microscope with 30 nm spatial resolution has been developed employing the third diffraction order of a zone plate objective. The microscope utilizes a capillary type condenser with suitable surface figure to generate a hollow cone illumination which is matched in illumination range to the numerical aperture of the third order diffraction of a zone plate with an outmost zone width of 50 nm. Using a test sample of a 150 nm thick gold spoke pattern with finest half-pitch of 30 nm, the authors obtained x-ray images with 30 nm resolution at 8 keV x-ray energy. © 2006 American Institute of Physics. [DOI: 10.1063/1.2397483]

The resolution of a full-field-type transmission x-ray microscope^{1–4} (TXM) mainly depends on the width of the outmost zones of the objective zone plate.^{5–8} In the soft x-ray region (100 eV–1 keV), it has been reported that zone plate based TXM has achieved a spatial resolution of 15 nm,⁹ which is the highest resolution microscopic image demonstrated using electromagnetic radiation. Because of the decrease of the refractive index with x-ray energy, a phase zone plate operating in the hard x-ray regime (>1 keV) requires a much larger thickness of the zone structures than for the soft x-ray regime to generate an adequate phase shift and therefore practical focusing efficiency. The manufacture of a high resolution zone plate with small zone width operating in the hard x-ray regime is significantly more challenging, because the required aspect ratio (defined as the ratio of the zone thickness to the zone width) is much larger. High spatial resolution requires narrow widths of the outmost zones, which correspond to a larger diffraction angle and therefore higher numerical aperture, which is still hard to fabricate in an ideal zone plate in hard x rays.¹⁰

By using higher order diffraction of a zone plate (such as the third diffraction order),^{7,11,12} the resolution of the x-ray microscope can be increased significantly, since the numerical aperture of the zone plate increases proportionally to the diffraction order used. However, in the previous studies^{7,11,12} zone plates were used as a probe forming lens using coherent illumination, and not as microscope objectives in a full-field imaging geometry demonstrating the decrease in spot size and resolution. The increased resolution is also directly applicable to full-field transmission x-ray microscopy, but has been hampered in the past by the fact that no suitable x-ray condensers were available to illuminate the objective zone plate with an appropriate hollow cone illumination that is

matched to the numerical aperture of the objective zone plate used in the third diffraction order. The use of zone plates as condenser lenses is impractical due to the loss of efficiency when used in the third diffraction order.

In this letter, we report a demonstration of effective utilization of the third diffraction order of a zone plate objective by using a capillary condenser to provide an illumination beam that is matched in numerical aperture to the zone plate objective.

The complex transmission function of a pure phase zone plate $ZP(x,y)$ in the following equation is expanded with a modification according to that given by Schneider:¹

$$ZP(x,y) = \exp\left(-i\pi\left(\frac{1}{2} + \frac{2}{\pi} \sum_{m=1,3,5,\dots}^{\infty} C_m \sin\left[\frac{m\pi(x^2+y^2)}{\lambda f}\right]\right)\right). \quad (1)$$

The cross section of the zone plate is assumed to be of rectangular shape, and can be regarded as composed of different orders of lens with focus length of f/m . λ is the wavelength and f is the focus length of the zone plate. The x and y are Cartesian coordinates, and this function describes the phase retardation in two dimensions for a zone plate. The C_m in the Eq. (1) is equal to $1/m$ for a rectangular shape of zone plate. The term $1/2$ represents the zeroth order of the zone plate, and $m=1,3,5,\dots$, represents the first, third, fifth, and so on, harmonic, which give rise to the corresponding diffraction orders (positive and negative). The higher the diffraction order, the shorter is the focal length, and the larger the numerical aperture (NA) becomes. The spatial resolution δ of the zone plate is given by $\delta = K_1 \lambda / NA$, where the K_1 ranges from 0.3 to 0.61,⁹ depending on the illumination condition. The described TXM has a hollow cone illumination corresponding to partially coherent imaging. Our experi-

^{a)}Electronic mail: geyin@nsrrc.org.tw

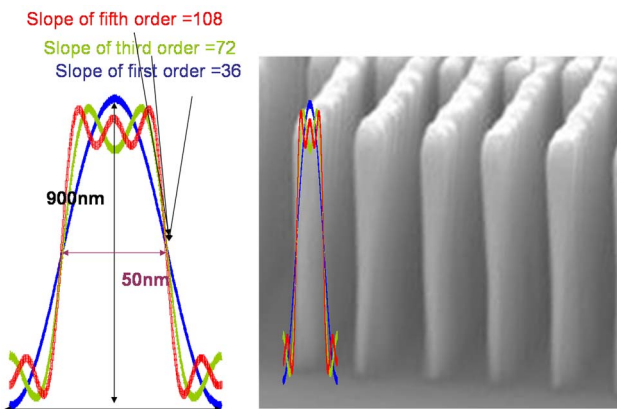


FIG. 1. (Color online) Left: The profile of the outmost zone of the zone plate. The vertical and horizontal axes are both in nanometer but in different scales. The blue, green, and purple lines indicate the profile of the first order, third order, and fifth order of the zone plate, respectively. The red line is the mixture between the first order and third order. Right: A SEM image showing the cross section of a zone plate which has a similar aspect ratio as the zone plate used in the experiment. The comparison shows that the slope of the zone plate is sharper than required (blue lines).

ments, which are described below, show that the value of K_1 achieved by our current setup is 0.45 using the first diffraction order of the zone plate.

The NA of a zone plate can be written as $NA_{\text{zone plate}} = m\lambda/2\Delta r$,¹ where λ is the wavelength, Δr is the outermost zone width of the zone plate, and $m=1,3,5$, etc., the diffraction order of the zone plate. For optimized, partially coherent illumination conditions in the TXM, the value of K_1 can be as small as 0.3 (Ref. 9) such that the theoretical spatial resolution of the third order image for optimized hollow cone illumination becomes $\delta=0.61\Delta r/m$. For a partially coherent illumination in our x-ray microscope, which uses a wider range of illumination angles, the value of K_1 has been determined to be 0.45. Therefore the expected resolution using the third diffraction order may be estimated to be $\delta=0.9\Delta r/m$. For the described x-ray microscope, we are using the diffraction order m equal to 3, and Δr is 50 nm; hence the resolution for this hollow cone-beam system should be close to 15 nm spatial resolution.

The zone profile directly determines the diffraction efficiency of each diffraction order. In Eq. (1), the C_m is the weight coefficient of each spatial frequency into which the zone plate grating is decomposed and represents the relative weight of each diffraction order. Analogous to Eq. (1), we can expand the zone plate profile function in a series as shown in Eq. (2), where the symbol h is the (constant) thickness of the zone plate and r is $\sqrt{x^2+y^2}$. As illustrated in Fig. 1 and Eq. (2), each higher order term m that contributes to the series adds to the sharpness of the zone edge, which means, in turn, that higher order diffraction only appears if the edge of the zone is sharp enough.

$$ZP_{\text{profile},m}(r) = h \left(\frac{1}{2} + \frac{2}{\pi} \sum_{m=1,3,5,\dots}^{\infty} \frac{1}{m} \sin \left[\frac{m\pi r^2}{\lambda f} \right] \right), \quad (2)$$

Figure 1 illustrates the variation of the zone profile slope for increasing diffraction orders m . The maximum slope depends on two parameters; the zone plate thickness h (900 nm for our case) and the outmost zone width Δr (50 nm for our case). (In fact, π is the optimal phase shift for a perfect Fresnel phase zone plate, as indicated in Eq. (1); it is the

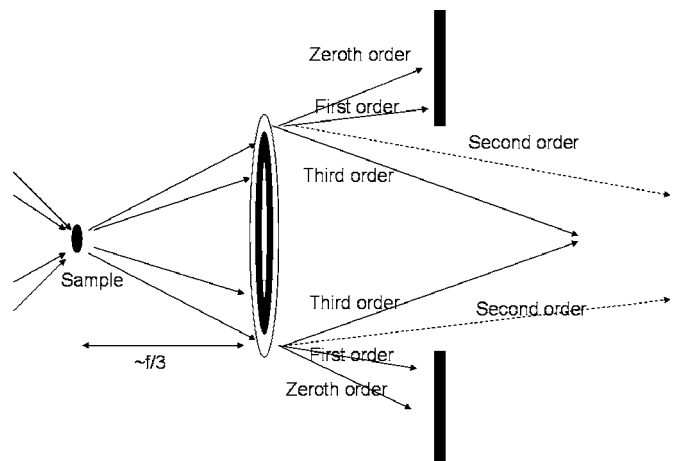


FIG. 2. This is the setup of third order image. A condenser lens is used to focus the beam at sample position and generate a hollow cone beam which matches the numerical aperture of the third order of the zone plate. After the beam passes through the zone plate, it is then diffracted to several different orders. The third order image can be decoupled with low order image and the third order image, and the images of low orders are blocked by a pinhole before the detector.

trade-off between diffraction efficiency and resolution.) The first order diffraction efficiency of the zone plate used in our experiment is measured to be above 10% and the third order efficiency is around 1%. The zone plate we are employing has a total of 425 zones and a diameter of 85 μm . However, we show in the Fig. 1 images of a grating fabricated with the same processes as the zone plate, but having different parameters. The image shows the profile of an outmost zone with the same aspect ratio of 18, and it can be seen that the slope of the edge appears to be sharper than what is required for third order imaging.

To achieve a third order imaging field free of other diffraction orders at the imaging plane, a suitable hollow cone illumination is used to match the numerical aperture of the zone plate used in the third diffraction order, as shown schematically in Fig. 2. The source of our TXM is the same as a previous report.⁴ Energy resolving power better than 1000 at 8 keV is employed to match the temporal coherence requirement of the zone plate, which states that the resolving power of the monochromator must be equal or exceed the zone number of the objective zone plate times the used diffraction order, which is 1275 for third order.¹³ The illumination cone angle ranges from 2.7 to 3.3 mrad generated by a capillary-based condenser with hyperbolic surface figure,^{14,15} producing a focus at the sample position with a size of about 15 μm in diameter. The distance between sample and zone plate is close to one-third of the designed focal length of the first diffraction order, which is about 9 mm. The field of view is $5 \times 5 \mu\text{m}^2$ in third order and the image distance is 1.2 m. Thus, the x-ray optical magnification is about 135 times. A high-resolution x-ray detector based on a scintillator screen with optical coupling to a charge-coupled device camera is employed to detect the x-ray image.

The test sample for our experiments is a Siemens star of 150 nm thickness with finest structures of 30 nm, which is fabricated out of electroplated gold on a silicon nitride membrane.¹⁰ This test sample exhibits an absorption of 6% (Ref. 16) in the gold features. This pattern is a spoke pattern, which has a narrower linewidth in the inner part than in the outer part. The modulation transfer function (MTF) of the

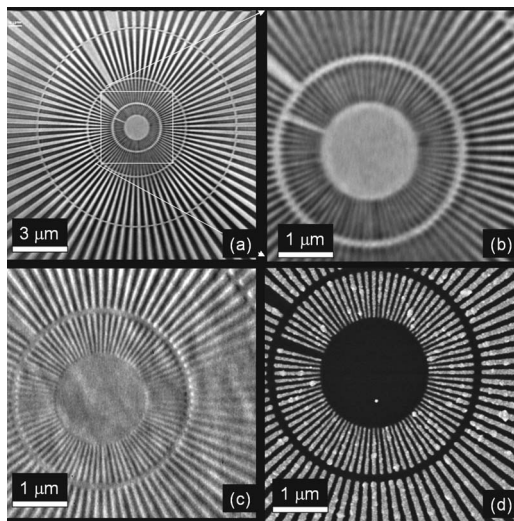


FIG. 3. Spoke pattern are imaged under different image modes: (a) by first order, (b) enlarged first third order, (c) by third order, and (d) by SEM. The area marked by a white square in Fig. 2(a) is the field of view of the third order image. The finest structure is in the center of the Siemens star. The third order image represents more details than the first order.

microscope can be deduced by measuring the contrast as a function of linewidth. The images of first order and third order of this test sample are used to estimate the spatial resolution of using the first and third diffraction orders of the zone plate, as shown in Fig. 3. Figures 3(b) and 3(c) show the same area with a field of view of $4.5 \times 4.5 \mu\text{m}^2$ in order to have a clear comparison showing the enhancement of the spatial resolution. The inner line of the spoke pattern is clearly resolved in the third order image, but is fuzzy in the first order image. The third order image shows that the half-pitch of 30 nm is clearly resolved. In order to obtain the MTF of the images, the modulation is calculated by the Michelson fringe visibility, which is given by $\nu = (I_{\max} - I_{\min}) / (I_{\max} + I_{\min})$. The Michelson visibility is measured in the different portions in images 3(b) and 3(c) for different spatial frequencies. After obtaining the visibility, the data are normalized with maximum visibility. The MTFs are plotted for both third and first order images as shown in Fig. 4. The maximum modulation in the vertical axis is normalized to 6% of absorption. The cutoff frequency for the first order is found at 22.5 lines/ μm , which is close to 45 nm and this gives the formula $\delta = 0.9\Delta r/m$. However, the cutoff frequency of the third order cannot be measured in this plot, since the modulation does not reach the bottom of the vertical axis. The cutoff frequency is obviously beyond the 33 lines/ μm , which is the spatial resolution of 30 nm. The interception of extension of the MTF with the noise background can be estimated as the spatial resolution of this TXM, which is about 37 lines/ μm , corresponding to a spatial resolution of 27 nm.

The exposure time for the image using third order is about 10 min and the exposure time of the image using first order is about 60 s. This is explained by the drop in diffraction efficiency by a factor of 10 between first order and third order, which agrees well with the theoretical predictions.

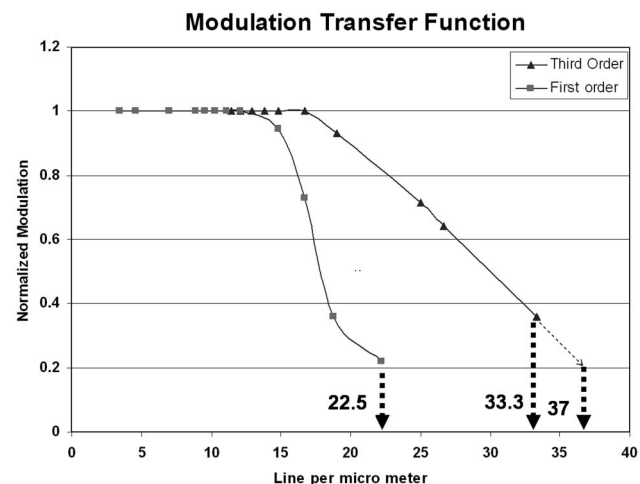


FIG. 4. Modulation transfer functions for third order and first order images. The resolution for first order is found to be 22.5 lines/ μm , which is the spatial resolution of 45 nm. The resolution for third order is estimated to be 37 lines/ μm , which is the spatial resolution of 27 nm.

In summary, the presented work takes advantage of using a reflective capillary condenser with high reflection efficiency which generates a hollow cone illumination that is matched to the numerical aperture of the zone plate used in third diffraction order, decoupling contributions of the first and third diffraction orders in the image. The third order image of the zone plate in transmission x-ray microscope is at 8 keV and resolution is 30 nm.

The authors thank Chris Jacobsen for valuable discussion and the contribution of the analysis software for estimation of the microscope resolution.

¹Gerd Schneider, Ultramicroscopy **75**, 85 (1998).

²U. Neuhausler, G. Schneider, W. Ludwig, and D. Hambach, J. Phys. D **36**, 79 (2003).

³W. Meyer-Ilse, H. Medecki, J. T. Brown, J. Heck, E. Anderson, C. Magowan, A. Stead, T. Ford, R. Balhorn, C. Petersen, and D. T. Attwood, *X-ray Microscopy and Spectromicroscopy* (Springer, Berlin, 1997).

⁴G. Yin, M. Tang, Y. Song, F. Chen, F. W. Duewer, W. Yun, C. Ko, H. D. Shieh, and K. S. Liang, Appl. Phys. Lett. **88**, 241115 (2006).

⁵E. Di Fabrizio, F. Romanato, M. Gentili, S. Cabrini, B. Kaulich, J. Susini, and R. Barrett, Nature (London) **401**, 895 (1999).

⁶B. Lai, W. B. Yun, D. Legnini, Y. Xiao, J. Chrzas, and P. J. Vidcaro, Appl. Phys. Lett. **61**, 1877 (1992).

⁷W. Yun and B. Lai, Rev. Sci. Instrum. **70**, 3537 (1999).

⁸W. Yun, B. Lai, Z. Cai, J. Maser, D. Legnini, E. Gluskin, Z. Chen, A. A. Krasnoperova, Y. Vladimirska, F. Cerrina, E. Di Fabrizio, and M. Gentili, Rev. Sci. Instrum. **70**, 2238 (1999).

⁹W. Chao, B. D. Harteneck, J. Alexander Liddle, Erik H. Anderson, and David T. Attwood, Nature (London) **435**, 1210 (2005).

¹⁰Xradia Inc., <http://www.xradia.com>

¹¹A. Takeuchi, Y. Suzuki, and H. Takano, J. Synchrotron Radiat. **9**, 115 (2002).

¹²Y. Suzuki, A. Takeuchi, H. Takano, and H. Takenaka, Jpn. J. Appl. Phys. **44**, 1994 (2005).

¹³M. Young, J. Opt. Soc. Am. **62**, 972 (1972).

¹⁴B. Murphy, D. L. White, Alastair A. MacDowell, and Obert R. Wood, Appl. Opt. **32**, 6920 (1993).

¹⁵D. H. Bilderback, D. J. Thiel, R. Pahl, and K. E. Brister, J. Synchrotron Radiat. **1**, 37 (1994).

¹⁶Center of X-ray Optics, <http://www-cxro.lib.gov>

¹⁷C. Jacobsen, S. Williams, E. Anderson, M. T. Browne, C. J. Buckley, D. Kern, J. Kirz, M. Rivers, and X. Zhang, Opt. Commun. **86**, 351 (1991).